


RESEARCH

Open Access



Na⁺/Ca²⁺ exchanger isoform 1 takes part to the Ca²⁺-related prosurvival pathway of SOD1 in primary motor neurons exposed to beta-methylamino-L-alanine

Tiziana Petrozziello¹, Francesca Boscia¹, Valentina Tedeschi¹, Anna Pannaccione¹, Valeria de Rosa¹, Angela Corvino², Beatrice Severino², Lucio Annunziato³ and Agnese Secondo^{1*} 

Abstract

Background: The cycad neurotoxin beta-methylamino-L-alanine (L-BMAA), one of the environmental trigger factor for amyotrophic lateral sclerosis/Parkinson-dementia complex (ALS/PDC), may cause neurodegeneration by disrupting organellar Ca²⁺ homeostasis. Through the activation of Akt/ERK1/2 pathway, the Cu,Zn-superoxide dismutase (SOD1) and its non-metallated form, ApoSOD1, prevent endoplasmic reticulum (ER) stress-induced cell death in motor neurons exposed to L-BMAA. This occurs through the rapid increase of intracellular Ca²⁺ concentration ([Ca²⁺]_i) in part flowing from the extracellular compartment and in part released from ER. However, the molecular components of this mechanism remain uncharacterized.

Methods: By an integrated approach consisting on the use of siRNA strategy, Western blotting, confocal double-labeling immunofluorescence, patch-clamp electrophysiology, and Fura 2-/SBFI-single-cell imaging, we explored in rat motor neuron-enriched cultures the involvement of the plasma membrane proteins Na⁺/Ca²⁺ exchanger (NCX) and purinergic P₂X₇ receptor as well as that of the intracellular cADP-ribose (cADPR) pathway, in the neuroprotective mechanism of SOD1.

Results: We showed that SOD1-induced [Ca²⁺]_i rise was prevented neither by A430879, a P₂X₇ receptor specific antagonist or 8-bromo-cADPR, a cell permeant antagonist of cADP-ribose, but only by the pan inhibitor of NCX, CB-DMB. The same occurred for the ApoSOD1. Confocal double labeling immunofluorescence showed a huge expression of plasmalemmal NCX1 and intracellular NCX3 isoforms. Furthermore, we identified NCX1 reverse mode as the main mechanism responsible for the neuroprotective ER Ca²⁺ refilling elicited by SOD1 and ApoSOD1 through which they promoted translocation of active Akt in the nuclei of a subset of primary motor neurons. Finally, the activation of NCX1 by the specific agonist CN-PYB2 protected motor neurons from L-BMAA-induced cell death, mimicking the effect of SOD1.

*Correspondence: secondo@unina.it

¹ Division of Pharmacology, Department of Neuroscience, Reproductive and Odontostomatological Sciences, School of Medicine, "Federico II" University of Naples, Via S. Pansini 5, 80131 Naples, Italy
Full list of author information is available at the end of the article



© The Author(s) 2022. **Open Access** This article is licensed under a Creative Commons Attribution 4.0 International License, which permits use, sharing, adaptation, distribution and reproduction in any medium or format, as long as you give appropriate credit to the original author(s) and the source, provide a link to the Creative Commons licence, and indicate if changes were made. The images or other third party material in this article are included in the article's Creative Commons licence, unless indicated otherwise in a credit line to the material. If material is not included in the article's Creative Commons licence and your intended use is not permitted by statutory regulation or exceeds the permitted use, you will need to obtain permission directly from the copyright holder. To view a copy of this licence, visit <http://creativecommons.org/licenses/by/4.0/>. The Creative Commons Public Domain Dedication waiver (<http://creativecommons.org/publicdomain/zero/1.0/>) applies to the data made available in this article, unless otherwise stated in a credit line to the data.

Conclusion: Collectively, our data indicate that SOD1 and ApoSOD1 exert their neuroprotective effect by modulating ER Ca^{2+} content through the activation of NCX1 reverse mode and Akt nuclear translocation in a subset of primary motor neurons.

Keywords: L-BMAA, NCX1, SOD1, Calcium signaling, Neuroprotection, ApoSOD1

Background

Calcium (Ca^{2+}) imbalance is now considered one of the key elements of the neurodegenerative process occurring in amyotrophic lateral sclerosis (ALS), a fatal adult-onset disease characterized by progressive degeneration of both upper and lower motor neurons [1, 2]. Accordingly, during the disease progression, dysfunctional Ca^{2+} homeostasis may lead to misfolding of several proteins [3], thus facilitating their toxic aggregation. Importantly, organellar Ca^{2+} homeostasis, with particular respect to the endoplasmic reticulum (ER), is compromised in ALS preclinical models and is now considered a relevant pathogenic mechanism of the disease [4, 5]. About 20% of cases of familial form (fALS) and 2–7% of sporadic form of ALS (sALS) are caused by mutations in the gene encoding the cytosolic Cu,Zn-superoxide dismutase (SOD1). This makes *sod1* the second most frequently mutated gene after *C9orf72* in ALS Caucasian patients [6–8] (<http://alsod.iop.kcl.ac.uk/>). While mutated SOD1 accumulates as unfolded trimers causing motor neuron degeneration [9], dysfunctional secretion of native wild-type SOD1 may also favor the neurodegeneration in ALS [10]. In fact, a chronic intraspinal infusion of wild-type SOD1 significantly delays disease progression in transgenic animals carrying mutant human SOD1^{G93A} [10]. Furthermore, mutant SOD1 may induce ER stress by targeting several molecular components of ER-associated degradation (ERAD) machinery [11]. On the other hand, a rapid exposure to wild type SOD1 may protect motor neurons against ER stress induced by the beta-methylamino-L-alanine (L-BMAA) [12], one of the cycad toxins causing the Guamanian form of ALS [13]. Interestingly, the activation of Akt/ERK1/2 pathway via a transient $[\text{Ca}^{2+}]_i$ rise may underline the protective effect of SOD1 [12]. Mechanistically, this neuroprotective effect is independent from the catalytic activity of the enzyme, since the non-metallated form ApoSOD1, lacking dismutase activity, may induce protection of motor neurons from L-BMAA toxicity likewise SOD1 [12]. Therefore, considering that the neuroprotection exerted by SOD1 and ApoSOD1 may pass through a rapid and transient $[\text{Ca}^{2+}]_i$ increase, in the present study we investigated, by a pharmacological and siRNA approach, the involvement of the $\text{Na}^+/\text{Ca}^{2+}$ exchanger isoforms (NCXs), the cyclic adenosine diphosphate-ribose (cADPR) receptor and the purinergic receptor P_2X_7 , most of which are implicated

in the pathogenesis of ALS. Furthermore, the correlation between this neuroprotective increase in $[\text{Ca}^{2+}]_i$ and Akt activation has been investigated.

Methods

Reagents

Media, sera, and antibiotics for cell cultures were purchased from Life Technologies (Milan, Italy). Mouse monoclonal anti-p-Akt (#4051) and rabbit polyclonal anti-GRP78 (#3183) were from Cell Signaling Technology Inc. (Danvers, MA, USA). Rabbit polyclonal antibody against Akt1/2/3 (#sc-8312) was from Santa Cruz Biotechnology, Inc. (Dallas, TX, USA). Rabbit polyclonal antibody against NCX1 (#π11-13) was from Swant (Bellinzona, Switzerland), rabbit polyclonal anti-NCX3 antibody was done by Dr. K. Philipson (University of California, Los Angeles, CA, USA). Mouse monoclonal anti-SOD (#S2147), mouse monoclonal anti- α -tubulin (#T5168) and rabbit polyclonal anti-MAP2 (#M3696) antibodies were from Sigma-Aldrich (Milan, Italy). ECL reagents and nitrocellulose membranes were from GE Healthcare (Milan, Italy). SOD1, retinoic acid, L-BMAA, thapsigargin, ATP, H_2O_2 , 8-bromo-cADPR, MK801, CNQX, oligomycin, 2-deoxy-D-glucose, 2',7'-dichlorofluorescein diacetate (DCF-DA), PD98059, LY294002, and all other reagents were from Sigma-Aldrich (Milan, Italy). A430879 was a kind gift from Prof. S. Bruzzone (Department of Experimental Medicine, University of Genova, Genova, Italy). The inactive mutant HA-Aktk179M (Akt D-) plasmids were donated by Prof. P. Formisano ("Federico II" University of Naples, Naples, Italy). Fura-2/AM and SBFI/AM were from Life Technologies (Milan, Italy).

Rat primary motor neurons

Motor neuron-enriched cultures were obtained from the spinal cord of 12–14-day-old Wistar rat embryos and cultured as previously described [12, 14]. Cytosine β -D-arabinofuranoside hydrochloride (Ara-C, 10 μM) was added at 4 and 8 DIV (days in vitro) to prevent non-neuronal cell growth. Primary motor neurons were kept at 37 °C in a humidified 5% CO_2 atmosphere and used after 10–12 DIV. All the procedures were performed according to the experimental protocols approved by the Ethical Committee of "Federico II" University of Naples, Naples, Italy, and according to the guidelines and regulations by

Italian Ministry of Health (D.Lgs. March 4th, 2014 from Italian Ministry of Health and DIR 2010/63 from UE).

Hybrid cell line

NSC-34 motor neurons were grown in Dulbecco's Modified Eagles Medium (DMEM) containing 10% fetal bovine serum (FBS), 2 mM L-glutamine, 100 IU/ml penicillin, and 100 µg/ml streptomycin, and kept in a 5% CO₂ and 95% air atmosphere at 37 °C. Before each experiment, NSC-34 cells were differentiated in 10 µM retinoic acid for 48 h, thus triggering a typical neuronal phenotype [15].

SOD1 inactivation

SOD1 was incubated with 200 mM H₂O₂ in 25 mM sodium bicarbonate buffer (pH 7.5) for 2 h at room temperature (RT). At the end, the reaction was stopped by adding 1000 U/ml catalase for 30 min at 37 °C. Finally, SOD1 activity was measured by the SOD assay kit purchased from Sigma-Aldrich (Milan, Italy), as previously described [12].

[Ca²⁺]_i and [Na⁺]_i measurements

[Ca²⁺]_i was measured by single cell computer-assisted video-imaging in NSC-34 motor neurons and in primary motor neurons, as previously reported [16]. Results are presented as cytosolic Ca²⁺ concentration calculated by the equation of Grynkiewicz et al. [17, 18]. NCX activity was evaluated as Ca²⁺ uptake through the reverse mode by using a Na⁺-deficient *N*-methyl-D-glucamine (NMDG) solution (Na⁺-free) containing (in mM): 5.5 KCl, 147 NMDG, 1.2 MgCl₂, 1.5 CaCl₂, 10 glucose, and 10 HEPES (pH 7.4). The irreversible and selective inhibitor of the sarco(endo)plasmic reticulum Ca²⁺-ATPase (SERCA) thapsigargin (Tg; 1 µM) was added 10 min before the beginning of the recordings, as previously described [16]. NCX activity was calculated as Δ% of peak/basal [Ca²⁺]_i values after perfusion with a Na⁺-free solution. [Na⁺]_i measurement was performed by loading motor neurons with 10 µM SBFI/AM incubated in the presence of 0.02% pluronic acid for 1 h at 37 °C [19].

Patch-clamp electrophysiology

NCX currents (I_{NCX}) in motor neurons were recorded by patch-clamp technique in whole-cell configuration using the commercially available amplifier Axopatch200B and Digidata1322A interface (Molecular Devices), as previously described [16, 20, 21]. I_{NCX} was recorded starting from a holding potential of -60 mV up to a short-step depolarization at +60 mV (60 ms). A descending voltage ramp from +60 to -120 mV was applied. I_{NCX} recorded in the descending portion of the ramp (from +60 to -120 mV) was used to plot the

current-voltage (I-V) relation curve. The I_{NCX} magnitude was measured at the end of +60 mV (reverse mode) and at the end of -120 mV (forward mode), respectively. To isolate I_{NCX}, the same cells were recorded first for total currents and then for currents in the presence of Ni²⁺ (5 mM), a selective blocker of I_{NCX}. To obtain the isolated I_{NCX}, the Ni²⁺-insensitive unspecific currents were subtracted from the total currents (I_{NCX} = I_T - I_{NiResistant}) [16, 20, 21]. Motor neurons were perfused with external Ringer's solution containing the following (in mM): 126 NaCl, 1.2 NaHPO₄, 2.4 KCl, 2.4 CaCl₂, 1.2 MgCl₂, 10 glucose, and 18 NaHCO₃ (pH 7.4). Twenty millimolar tetraethylammonium (TEA), 50 nM tetrodotoxin (TTX), and 10 µM nimodipine were added to Ringer's solution to abolish potassium, sodium, and calcium currents. The dialyzing pipette solution contained the following (in mM): 100 K-gluconate, 10 TEA, 20 NaCl, 1 Mg-ATP, 0.1 CaCl₂, 2 MgCl₂, 0.75 EGTA, and 10 HEPES (pH 7.2). Membrane capacitance was calculated according to the following equation: C_m = τ_c · I_o / ΔE_m (1 - I_∞ / I_o), where C_m is membrane capacitance, τ_c is the time constant of the membrane capacitance, I_o is the maximum capacitance current value, ΔE_m is the amplitude of the voltage step, and I_∞ is the amplitude of the steady state current [19].

Immunocytochemistry

Motor neurons were cultured on glass coverslips for 12 days. Then, cells were rinsed twice in cold 0.01 M PBS (pH 7.4) and fixed in 4% (w/v) paraformaldehyde (Sigma-Aldrich, Milan, Italy) for 20 min at RT. After three washes in PBS, cells were blocked with 3% (w/v) BSA and 0.05% Triton-X (Bio-Rad, Milan, Italy) for 1 h at RT. Coverslips were then incubated overnight at 4 °C with the following primary antibodies: rabbit polyclonal antibody against NCX1 (#π11-13, Swant, Bellinzona, Switzerland), rabbit polyclonal antibody against NCX3 (Dr. K. Philipson Laboratory, University of California, Los Angeles, CA, USA), mouse monoclonal antibody against SOD (#S2147, Sigma-Aldrich, Milan, Italy), mouse monoclonal antibody against p-Akt (#4051, Cell Signaling Technology Inc., Danvers, MA, USA), or rabbit polyclonal antibody against MAP2 (#M3696, Sigma-Aldrich, Milan, Italy). After three washes in PBS, coverslips were incubated in the dark with the corresponding secondary antibodies for 1 h at RT. Dapi was used to stain nuclei. Images were acquired by using a Zeiss LSM 700 laser (Carl Zeiss) scanning confocal microscope.

Small interfering RNA

NCX1 and NCX3 knocking down was obtained by siRNA duplex against NCX1 or NCX3 and their non-targeting control (Qiagen, Milan, Italy), as previously described [22, 23]. MEK1 downregulation was achieved by using

a specific siRNA against MEK1 and its non-targeting Control (Dharmacon, Lafayette, CO, USA), as previously reported [12]. Motor neurons were transfected for 5 h with each duplex at a final concentration of 10 nM using HiPerFect transfection reagent (Qiagen, Milan, Italy).

L-BMAA treatment and cell viability measurement

Primary cultures of motor neurons were exposed to 300 μ M L-BMAA for 48 h. SOD1 (400 ng/ml) or ApoSOD1 (400 ng/ml) were added in fresh medium 10 min before L-BMAA addition, while the specific NCX1 activator, CN-PYB2 (10 nM) [24], was added in fresh medium together with the neurotoxin. After 48 h exposure to L-BMAA, mitochondrial activity was evaluated by the MTT (3[4,5-dimethylthiazol-2-yl]-2,5-diphenyl-tetrazolium bromide) assay. Data are expressed as a percentage of cell survival of control cultures.

Western blotting

After treatments, cells were lysed in ice-cold lysis buffer containing 20 mM Tris-HCl (pH 7.5), 10 mM NaF, 1 mM phenylmethylsulfonyl fluoride, 1% NONIDET P-40, 1 mM Na_3VO_4 , 0.1% aprotinin, 0.7 mg/ml pepstatin and 1 μ g/ml leupeptin. Protein concentration of each sample was determined by the Bradford method [25]. Proteins (50 μ g) were separated on 10% SDS-polyacrylamide gels and transferred onto Hybond ECL nitrocellulose membranes (GE Healthcare, Milan, Italy). Membranes were blocked with 5% non-fat dry milk in 0.1% Tween 20 (Sigma-Aldrich, Milan, Italy) (2 mM Tris-HCl and 50 mM NaCl, pH 7.5) for 2 h at RT and then incubated overnight at 4 °C in the blocking buffer containing the mouse monoclonal antibody against p-Akt (1:1000) or the rabbit polyclonal antibody against GRP78 (1:1000). Membranes were then re-blotted with the rabbit polyclonal antibody against Akt1/2/3 (1:1000) or with the mouse monoclonal anti- α -tubulin (1:2000) antibody. Immunoreactive bands were detected with the ECL reagent (GE Healthcare, Milan, Italy) and then the optical density of the bands was determined by Chemi-Doc Imaging System (Bio-Rad, Milan, Italy).

Chemical hypoxia

Chemical hypoxia was reproduced by adding to the NSC-34 cells 5 μ g/ml oligomycin (an oxidative phosphorylation inhibitor) plus 2-deoxy-D-glucose (a glycolysis inhibitor) in a glucose-free medium, containing (in mM): 145 NaCl, 5.5 KCl, 1.2 MgCl_2 , 1.5 CaCl_2 and 10 HEPES (pH 7.4) for 45 min. Control cells were exposed to a Normal Krebs medium, containing (in mM): 145 NaCl, 5.5 KCl, 1.2 MgCl_2 , 1.5 CaCl_2 , 10 glucose, and 10 HEPES (pH 7.4) for 45 min, as previously described [16].

Reactive oxygen species (ROS) production

2',7'-dichlorofluorescein diacetate (DCF-DA) was used to detect ROS production in differentiated NSC-34 motor neurons. At the end of the experiments, DCF-DA fluorescence was acquired by a Nikon Eclipse 400 microscope (Nikon Instruments) equipped with a CCD digital camera (Coolsnap-Pro, Media Cybernetics).

Statistical analysis

Data are expressed as mean \pm S.E.M. Statistical comparisons between controls and treated experimental groups were performed using the one-way ANOVA, followed by Newman-Keuls test. $P < 0.05$ was considered statistically significant.

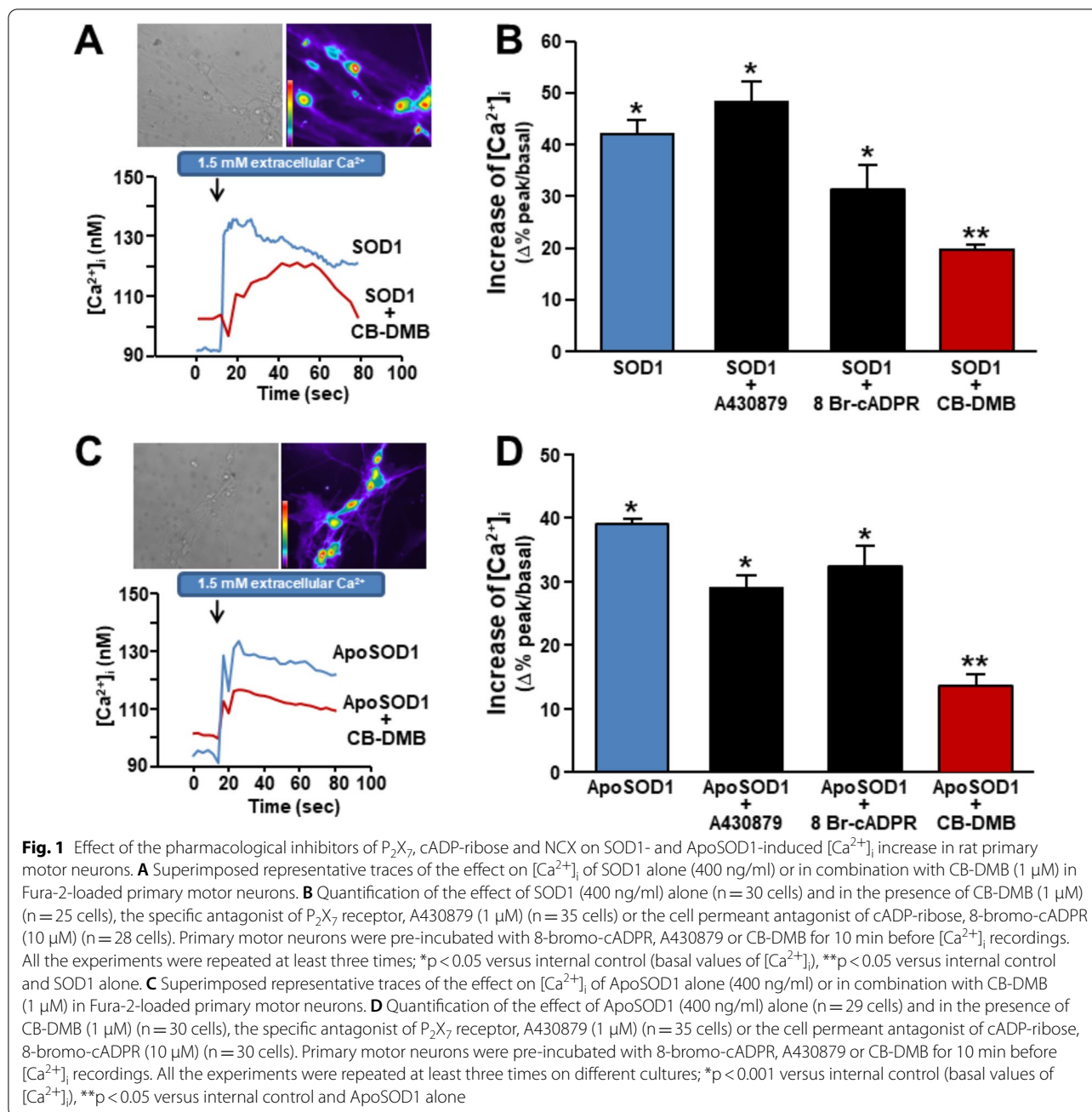
Results

Plasma membrane $\text{Na}^+/\text{Ca}^{2+}$ exchanger isoform 1 (NCX1) mediates a rapid $[\text{Ca}^{2+}]_i$ increase induced by SOD1 and ApoSOD1 in rat primary motor neurons

In consideration of the modulatory role exerted on Ca^{2+} signaling by purinergic P_2X_7 receptor [26], cADP-ribose receptor [27, 28], and $\text{Na}^+/\text{Ca}^{2+}$ exchanger (NCX) [29–31], rat primary motor neurons were exposed to SOD1 or ApoSOD1 in presence of their specific antagonists [32–34] A430879 (1 μ M), 8-bromo-cADPR (10 μ M), or CB-DMB (1 μ M). These pharmacological tools were used at the respective IC_{50} for the proposed targets. Our results indicated that only the NCX pan inhibitor CB-DMB significantly reduced the early increase of $[\text{Ca}^{2+}]_i$ induced by SOD1 (Fig. 1A, B) and ApoSOD1 (Fig. 1C, D). In contrast, A430879, blocking P_2X_7 , and the cell permeant 8-bromo-cADPR, that inhibits cADP-ribose action, did not modify SOD1- (Fig. 1B) and ApoSOD1-induced $[\text{Ca}^{2+}]_i$ rise (Fig. 1D). This may suggest the involvement of NCX in the upstream mechanism of SOD1 and ApoSOD1 and possibly highlights the participation of the exchanger in their prosurvival effects against L-BMAA toxicity.

The activation of NCX1 reverse mode induced by SOD1 and ApoSOD1 is due to the $[\text{Na}^+]_i$ accumulation in rat primary motor neurons

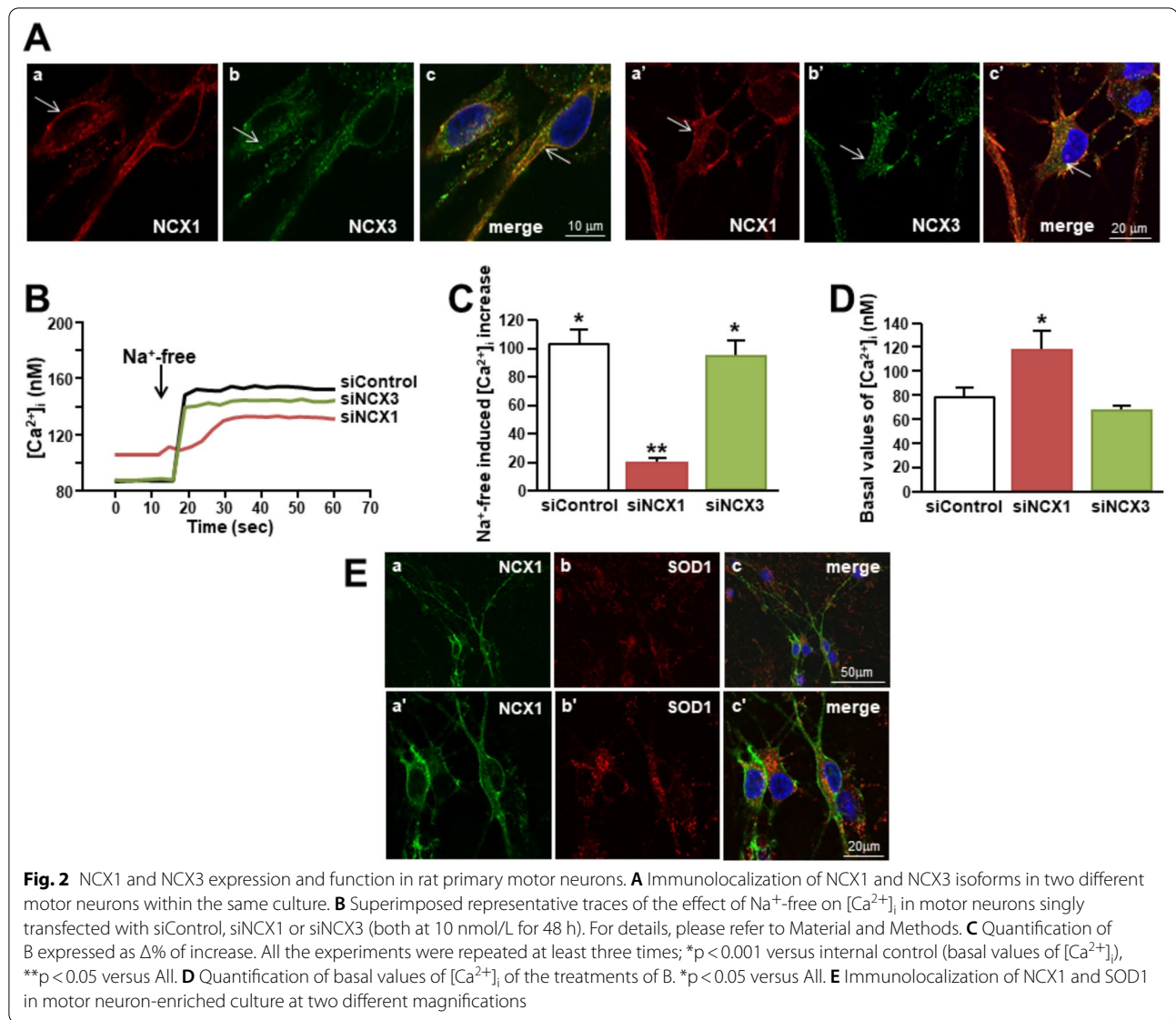
In order to identify which isoform of NCX was involved in the Ca^{2+} -dependent neuroprotective mechanism elicited by SOD1 and ApoSOD1, we analyzed the expression and activity of NCX1 and NCX3 isoforms in motor neuron-enriched cultures. As shown by confocal analysis in Fig. 2A, NCX1 and NCX3 isoforms were both significantly expressed in motor neurons. Of note, NCX1 was expressed in $\sim 100\%$ of MAP2-positive motor neurons of the enriched cultures, the $19\% \pm 2$ of which expressed NCX1 at higher level (Additional File 1). Interestingly,



NSC-34 cells significantly expressed the two exchanger isoforms with the same localization (Additional File 1). Of note, in these clonal motor neurons, SOD1 induced a significant increase in $[Ca^{2+}]_i$ that was prevented by the NCX inhibitor CB-DMB but not by AMPA and *N*-methyl-*D*-aspartate (NMDA) receptor inhibitors CNQX and MK801, respectively (Additional File 1).

However, in primary motor neurons and in differentiated NSC-34 cells, NCX1 was detected only on plasma membrane of the soma and neuronal processes, while

NCX3 was mostly present in the whole intracellular compartment (Fig. 2; Additional File 1). In primary motor neurons, the intracellular localization of NCX3 was prevalent in some motor neurons resembling motor neurons 2. Therefore, a clear co-localization between the two isoforms was only marginally observed (Fig. 2A; Additional File 1). Then, NCX activity was studied by exposing Fura-2/AM-loaded motor neurons to a Na^+ -free solution forcing the exchanger to operate in the reverse mode-mediated $[Ca^{2+}]_i$ increase (Fig. 2B, C). However,

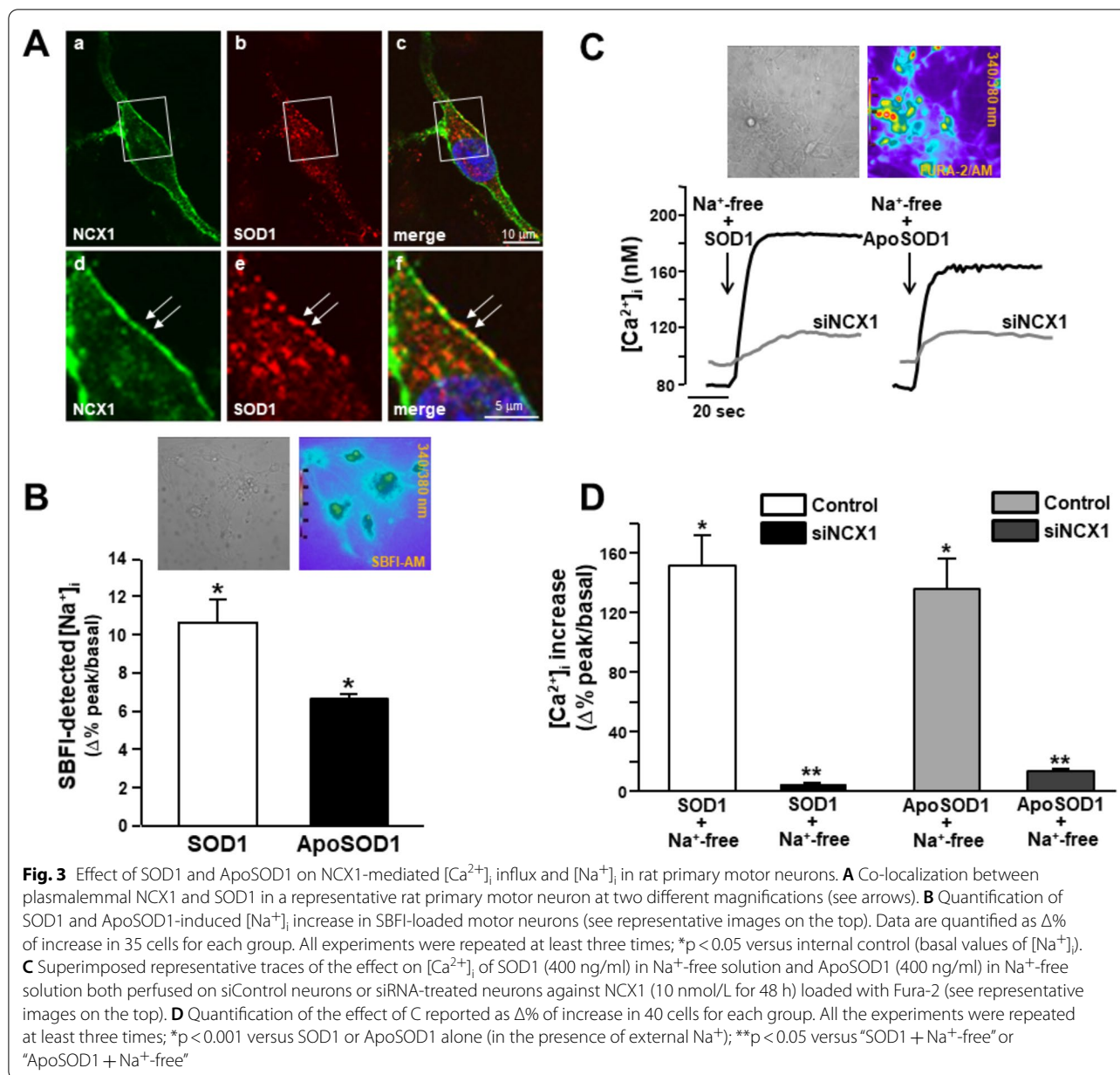


NCX1 knocking down produced by siNCX1 completely abolished Na⁺-free-induced [Ca²⁺]_i rise, while NCX3 knocking down did not (Fig. 2B, C). Interestingly, in siNCX1-treated neurons a significant increase of basal [Ca²⁺]_i was detected if compared to control (i.e. siControl-treated neurons) (Fig. 2D). Moreover, SOD1 immunosignal was detected in NCX1-positive motor neurons (Fig. 2E) in which a significant co-localization between NCX1 and endogenous SOD1 was observed sometimes at plasma membrane level (see arrows of Fig. 3A). Moreover, in SBF1-loaded motor neurons, SOD1 (400 ng/mL) induced a significant increase in [Na⁺]_i when compared to untreated controls (Fig. 3B). The same [Na⁺]_i rise was detected after a brief exposure to ApoSOD1 (400 ng/mL) (Fig. 3B).

Furthermore, NCX activity was potentiated by both SOD1 and ApoSOD1 added to a Na⁺-free solution compared with control neurons exposed to Na⁺-free alone (Fig. 3C, D). However, this Na⁺-free-dependent activation of NCX was abolished in motor neurons previously silenced for NCX1 (Fig. 3C, D).

NCX1 reverse mode induced by SOD1 and ApoSOD1 determines ER Ca²⁺ entry in rat primary motor neurons

To study the mechanism of action of SOD1, NCX current was recorded by patch-clamp electrophysiology in whole cell configuration (Fig. 4). SOD1, as well as its metal-free form ApoSOD1, determined a significant increase of NCX reverse mode measured at +60 mV (Fig. 4A–C). On the other hand, NCX forward mode, measured at

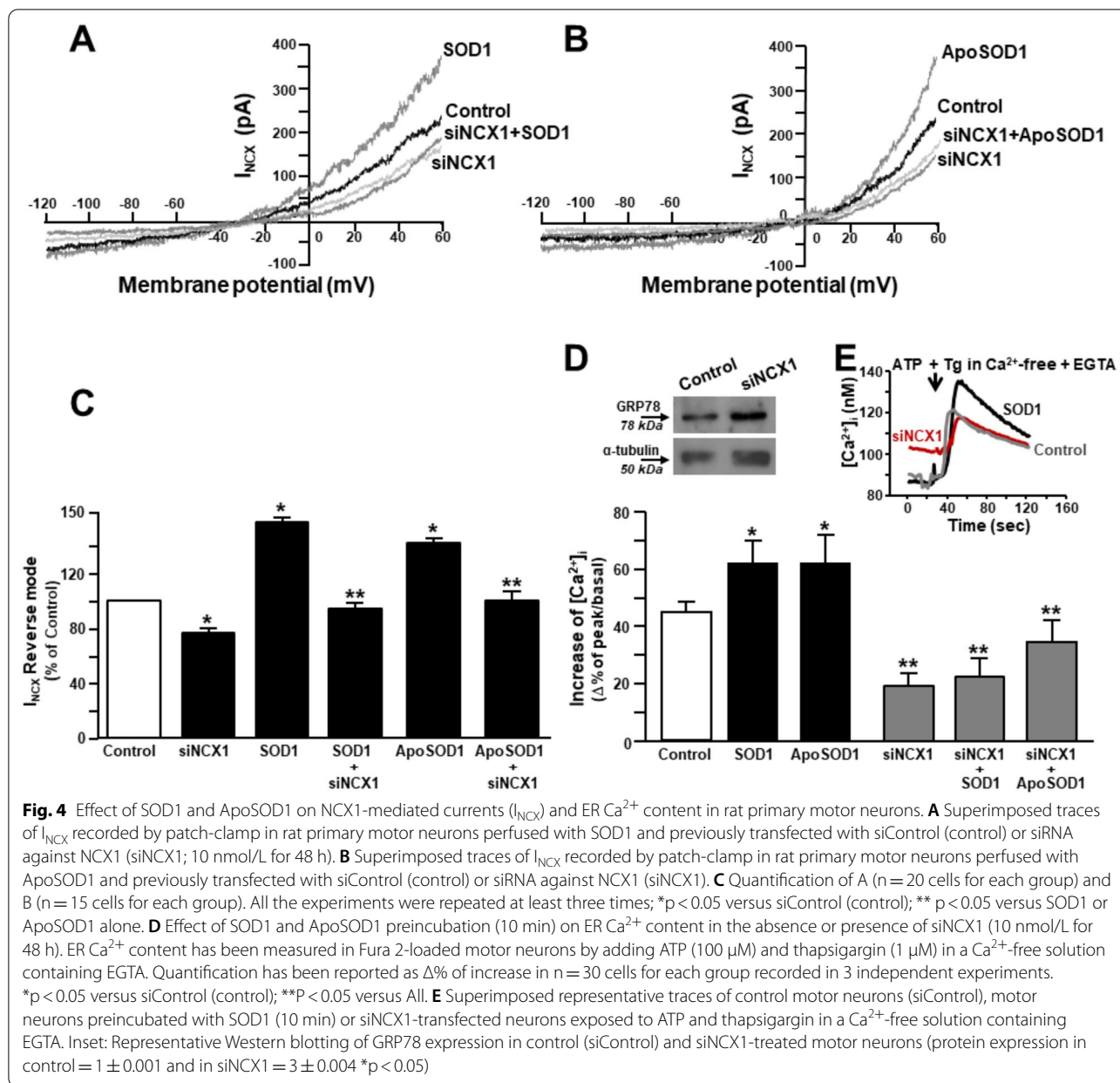


-120 mV, was unaffected by SOD1 or ApoSOD1 perfusion (Fig. 4A–C). Moreover, the knocking down of NCX1 by siNCX1 not only reduced NCX total current in motor neuron-enriched cultures but also counteracted the increase of NCX reverse mode induced by SOD1 (Fig. 4A, C) or ApoSOD1 (Fig. 4B, C). Of interest, the preincubation with SOD1 or ApoSOD1 enhanced ER Ca^{2+} content that was measured at cytosolic level as ER Ca^{2+} release after the perfusion with the sarco(endo)plasmic reticulum ATPase inhibitor thapsigargin (Fig. 4D, E). Interestingly, this SOD1-induced ER Ca^{2+} accumulation, as well as that produced by ApoSOD1, was prevented

by siNCX1 (Fig. 4D). Of note, siNCX1 reduced ER Ca^{2+} content above the control level (Fig. 4D). Accordingly, in siNCX1-treated motor neurons the ER stress marker GRP78 was upregulated compared with siControl (inset Fig. 4D).

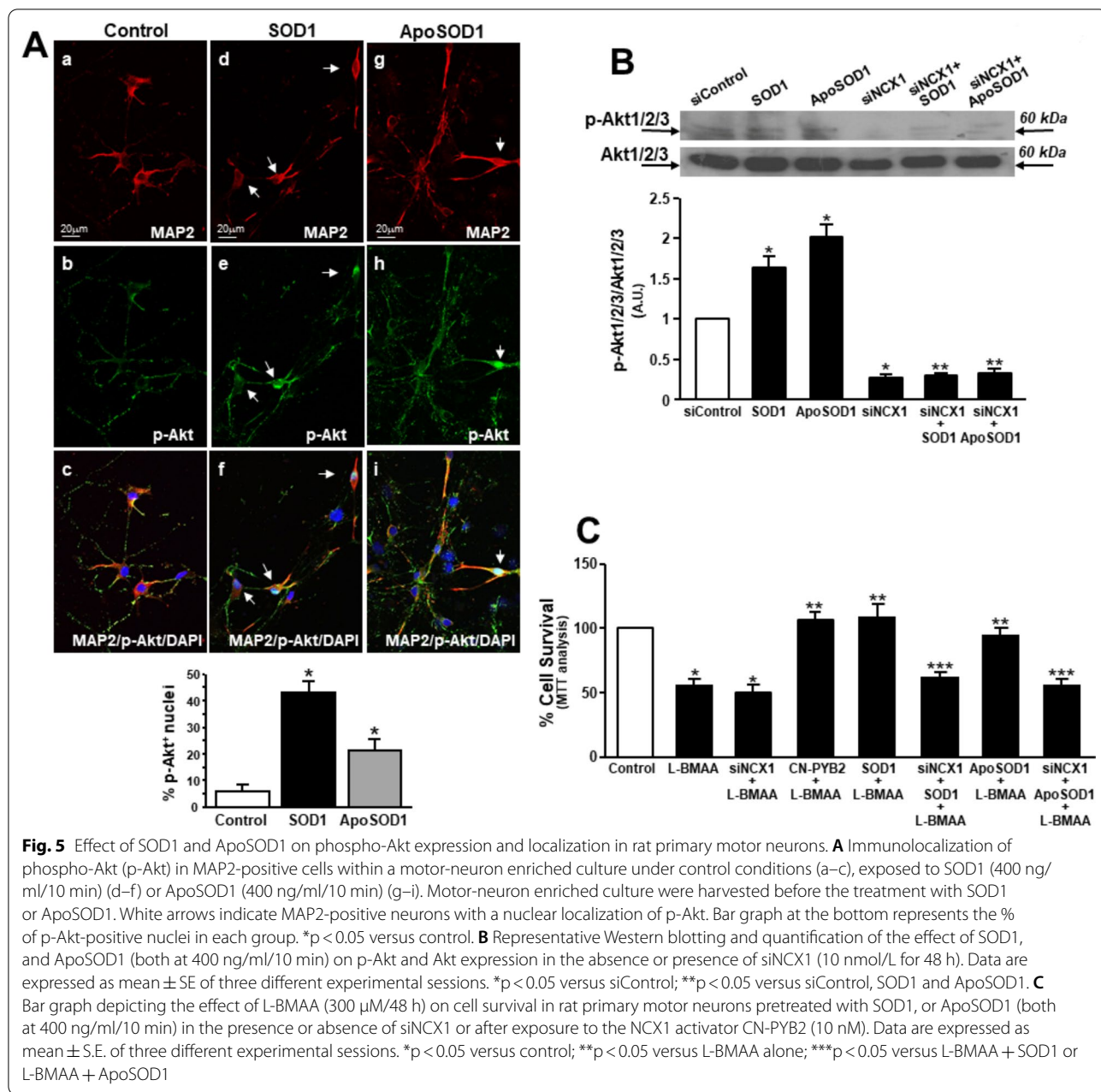
Nuclear localization and phosphorylation of Akt induced by SOD1 and ApoSOD1 depend on NCX1 activation

To clarify the role of NCX1 activation in SOD1 and ApoSOD1 neuroprotective mechanism, Akt localization and expression were studied in primary motor



neurons exposed to these molecules. Figure 5A shows a peculiar nuclear localization of active Akt (phospho-Akt; p-Akt) in a subset of MAP2-positive neurons exposed to SOD1 or ApoSOD1 for 10 min. Of note, this subset of motor neurons resembled those small group of cells expressing NCX1 at higher level (please see arrows in Additional File 1). Interestingly, Western blotting analysis showed that SOD1- and ApoSOD1-induced p-Akt overexpression was prevented in primary motor neurons silenced for NCX1 (Fig. 5B). In accordance with these results, siNCX1 prevented both SOD1 and ApoSOD1-induced neuroprotection

in primary motor neurons exposed to the neurotoxin L-BMAA (300 μ M/48 h) (Fig. 5C; Additional File 3). Of interest, L-BMAA may share the same detrimental mechanism with other cycad toxins inducing downstream mitochondrial dysfunction and reactive oxygen species (ROS) production [35, 36]. Therefore, the effect of SOD1 was tested also in motor neurons exposed to chemical hypoxia, a stimulus for ROS generation (Additional File 2). In this model, SOD1 prevented cell death in a concentration-dependent way by stimulating MEK1/PI3/K/Akt phosphorylation (Additional File 2). As previously demonstrated [12], this protective



pathway is activated also by SOD1 in motor neurons exposed to L-BMAA able to induce cell death in a concentration-dependent way (Additional File 3).

Indeed, the participation of NCX1 was further confirmed by the neuroprotective effect of the specific activator of the exchanger isoform CN-PYB2 [24] that prevented L-BMAA-induced cell death in motor neuron-enriched cultures (Fig. 5C).

Collectively, our results demonstrated the important role played by NCX1 in triggering SOD1- and

ApoSOD1-dependent prosurvival pathway through an increase of $[Ca^{2+}]_i$.

Discussion

With the aim to identify new druggable targets in ALS, the present study provides a comprehensive analysis of the upstream mechanisms underlying SOD1-induced neuroprotection in an in vitro model of the disease. Here, we tested the involvement of P_2X_7 , NCX, and cADPR, three ionic proteins mainly involved in neuronal $[Ca^{2+}]_i$ handling and possibly mediating the toxic

effect of L-BMAA. For instance, the lack of P_2X_7 aggravates ALS symptoms by determining gliosis and motor neuron death [37–41]. Furthermore, NCX dysfunction intervenes in ALS pathogenesis while its activation may prolong life span of SOD1^{G93A} mice through the attenuation of motor neuron loss [31, 42]. On the other hand, cADPR causes Ca^{2+} mobilization [43] through a direct or indirect release from ER [44]. Moreover, in L-BMAA-treated cultures SOD1 produced neuroprotective effects in a Ca^{2+} -related way and independently from its catalytic activity [12]. Accordingly, its free-metal form ApoSOD1 may mimic SOD1 effect in L-BMAA-treated cultures by promoting a Ca^{2+} -dependent activation of ERK1/2 and Akt and preventing ER stress-induced cell death [12]. Among the ionic mechanisms investigated, we identified the bi-directional ion transporter NCX1 as the unique protein underlying SOD1- and ApoSOD1-induced $[Ca^{2+}]_i$ increase and, therefore, involved in their prosurvival effects. Patch-clamp experiments revealed that SOD1 as well as ApoSOD1 promoted a rapid activation of NCX1 in the reverse mode of operation thus eliciting a significant increase in ER Ca^{2+} content. This possibly counteracted ER Ca^{2+} leak induced by L-BMAA thus delaying ER stress. Of particular interest is that NCX plays a crucial role against ER stress in other neurodegenerative disease including stroke and Alzheimer's disease [16, 19, 29, 30]. This seems to be due to the ability of the exchanger to counteract Ca^{2+} leak of the most relevant Ca^{2+} -storing organelle and, therefore, to hamper the transductional cascade of ER stress. In fact, in an in vitro model of stroke, augmented ER Ca^{2+} refilling was mediated by NCX1 working in the reverse mode [29]. The same may occur in cortical neurons exposed to ischemic preconditioning able to induce tolerance against a subsequent harmful stimulus [30]. This suggests that the antiporter is crucial for counterbalance the ER Ca^{2+} dysfunction induced by hypoxia in neurons. In accordance with this view, in the present study, NCX1 knocking down in primary motor neurons not only reduced ER Ca^{2+} content above the resting level but also induced the overexpression of GRP78, an indubitable ER stress marker. Moreover, the relevance of NCX1 at motor neuron level was confirmed by the neuroprotective effect exerted by the new selective pharmacological activator of NCX1, CN-PYB2 [24], in L-BMAA-treated motor neurons.

Besides its role in mediating the upstream Ca^{2+} increase, NCX expression is regulated by most of the transductional elements activated by SOD1 and ApoSOD1 in motor neurons [12, 45, 46]. On the other hand, by a feedback mechanism, the same transductional elements are modulated by NCX function [12, 47]. This is consistent with the possible long-lasting participation

of NCX1 in the transductional cascade underlying the neuroprotective effects of SOD1. In this context, our data showed a peculiar nuclear localization of active Akt in a subset of MAP2-positive neurons exposed to SOD1 as well as ApoSOD1. Interestingly, all Akt forms (i.e. Akt1/2/3) have been reported to reside in the nucleus or to migrate into the nucleus in response to a variety of protective stimuli in order to block apoptotic machinery or to induce the expression of those genes involved in cell survival [48].

Furthermore, we showed that in SBFI-loaded motor neurons, SOD1 as well as ApoSOD1 induced a significant increase in $[Na^+]_i$. In this respect, we reasoned that this ionic mechanism could be useful to drive SOD1-induced activation of NCX1 in the reverse mode of operation. Therefore, it is possible that SOD1 and ApoSOD1 interfered with the Na^+ -dependent NCX1 function by the modulation of other sodium transporters expressed in motor neuron plasma membrane. In this respect, reduced Na^+/K^+ ATPase- $\alpha 3$ activity has been observed in animal models of ALS as well as its reduced levels in the spinal cord of both sporadic and familial ALS patients [49]. In addition, the pharmacological inhibition of Na^+/K^+ ATPase- $\alpha 3$ is able to worsen disease pathology, thus confirming that an early Na^+ -dependent hyperexcitability is neuroprotective in ALS [50].

Collectively, this study shows that the initial phase of the complex mechanism shared by SOD1 and its non-metalled form ApoSOD1 in ALS/PDC model passed through the activation of NCX1 reverse mode/ER Ca^{2+} refilling and nuclear Akt activation.

Conclusions

In the present study the Na^+/Ca^{2+} exchanger isoform 1 (NCX1) has been identified as the main upstream mechanism underlying the non-enzymatic and neuroprotective action of SOD1 in an in vitro model of ALS. Molecularly, P_2X_7 receptor and cADP-ribose receptor are not involved in this neuroprotective mechanism. Under basal conditions, a significant co-localization between NCX1 and endogenous SOD1 was observed at plasma membrane level in a motor neuron-enriched culture. Transductionally, SOD1 and ApoSOD1 elicited the activation of NCX1 in the reverse mode of operation favoring Ca^{2+} influx via a previous increase in $[Na^+]_i$. Then, NCX1 recharged ER of Ca^{2+} protecting from ER stress and determining Akt phosphorylation and its nuclear translocation in a subset of primary motor neurons. Furthermore, pharmacological activation of NCX1 protected motor neurons from the toxic effect of L-BMAA thus showing a good profile as a new candidate for pioneering ALS treatment.

Abbreviations

[Ca²⁺]_i: Intracellular calcium concentration; ER: Endoplasmic reticulum; SOD1: Cu,Zn-superoxide dismutase; NCX1: Na⁺/Ca²⁺ exchanger isoform 1; NCX3: Na⁺/Ca²⁺ exchanger isoform 3; I_{NCX}: NCX currents; L-BMAA: Hydrochloride/β-N-methylamino-L-alanine; ALS: Amyotrophic lateral sclerosis; MT: 3-(4,5-Dimethylthiazol-2-yl)-2,5, diphenyltetrazolium bromide; Fura-2: (1-[2-(5-Carboxyoxal-2-yl)-6-aminobenzofuran-5-oxyl]-2-(2'-amino-5'-methylphenoxy)-ethane-N,N,N',N'-tetraacetic acid); SBFI-AM: 1,3-Benzenedicarboxylic acid, 4,4'-[1,4,10-trioxo-7,13-diazacyclopentadecane-7,13-diylbis(5-methoxy-6,12-benzofurandiyl)]bis-,tetrakis[(acetyloxy)methyl] ester.

Supplementary Information

The online version contains supplementary material available at <https://doi.org/10.1186/s12964-021-00813-z>.

Additional file 1. (A) Immunolocalization of NCX1 (a,d) and MAP2 (b,e) within a motor-neuron enriched culture under control conditions. Nuclei were stained with nuclear DNA stain 4, 6-diamino-2-phenylindole (DAPI). Arrows indicate MAP2-positive cells with higher level of NCX1 expression. **(B)** Immunolocalization of NCX1 and NCX3 in differentiated NSC-34 cells. **(C)** Quantification of SOD1-induced [Ca²⁺]_i in presence of CNQX (20 μM), MK801 (10 μM), or CB-DMB (1 μM) in motor neurons expressed as Δ% of increase. All the experiments were repeated at least three times on at least 35 cells for each group; **p* < 0.001 vs control (basal values of [Ca²⁺]_i).

Additional file 2. (A) Bar graph depicting the effect of Chemical Hypoxia on cell survival of differentiated NSC-34 cells pretreated (10 min) with 40, 400 or 4000 ng/ml SOD1. Data are expressed as mean±S.E. of three different experimental sessions. **p*<0.05 versus control; ***p*<0.05 versus Chemical Hypoxia alone and ****p*<0.05 versus All. **(B)** DCF-DA-detected ROS production in differentiated NSC-34 cells exposed to Chemical Hypoxia or Chemical Hypoxia plus SOD1 (400 ng/ml). Data are expressed as mean±S.E. of three different experiments. **p*<0.05 versus control; ***p*<0.05 versus Chemical Hypoxia alone. **(C)** Bar graph depicting the effect of Chemical Hypoxia on cell survival of differentiated NSC-34 motor neurons transfected with siMEK1 (10 nM) or treated with PD98059, or Akt D— (2 μg/μl) or treated with LY294002 and then exposed to SOD1 (400 ng/ml/10 min). Data are expressed as mean±S.E. of three different experimental sessions. **p*<0.05 versus control alone; ***p*<0.05 versus Chemical Hypoxia alone; ****p*<0.05 versus Chemical Hypoxia +SOD1.

Additional file 3. Bar graph depicting the effect of L-BMAA (0.01-1 mM) on cell survival of differentiated NSC-34 cells. Data are expressed as mean±S.E. of three different experimental sessions. **p*<0.05 versus control or 0.01 mM and 0.1 mM L-BMAA; ***p*<0.05 versus control and all previous concentrations.

Acknowledgements

The authors would thank Francesco Frecentese and Ferdinando Forino for participating to the synthesis of CN-PYB2.

Authors' contributions

Conceptualization: A.S.; Methodology: T.P., V.T., V.d.R., A.P., F.B. Formal Analysis: V.T., F.B.; Investigation: A.S., V.T., V.d.R., T.P.; A. P. Data Curation: T.P., A.S., V.T., F.B. CN-PYB2 synthesis: B.S.; A.C. Writing-Original Draft Preparation: A.S.; T.P., F.B.; Writing-Review & Editing, A.S., L.A. Funding Acquisition, A.S. All authors read and approved the final manuscript.

Funding

This work was supported by the Italian Ministry of Education, University and Research (PRIN2015–Prot. 2015KRY5JN), Progetto Speciale di Ateneo (CA.04_CDA_n_103 27.03.2019) and FRA.Linea.A.2020 (DR.2020.2449) to A.S.

Availability of data and materials

All raw data are available on request.

Declarations

Ethics approval and consent to participate

All the procedures were performed according to the experimental protocols approved by the Ethical Committee of “Federico II” University of Naples, Italy, and according to the guidelines and regulations by Italian Ministry of Health (D.Lgs. March 4th, 2014 from Italian Ministry of Health and DIR 2010/63 from UE). The authors declare consent to participate.

Consent for publication

Not applicable.

Competing interests

The authors declare no competing interests.

Author details

¹Division of Pharmacology, Department of Neuroscience, Reproductive and Odontostomatological Sciences, School of Medicine, “Federico II” University of Naples, Via S. Pansini 5, 80131 Naples, Italy. ²Department of Pharmacy, School of Medicine, “Federico II” University of Naples, Via D. Montesano 49, 80131 Naples, Italy. ³IRCCS SDN, Via E. Gianturco 113, 80143 Naples, Italy.

Received: 23 July 2021 Accepted: 2 December 2021

Published online: 12 January 2022

References

1. Chou SM. Pathology-light microscopy of amyotrophic lateral sclerosis. In: Smith RA, editor. Handbook of amyotrophic lateral sclerosis. New York: Marcel Dekker; 1992. p. 133–81.
2. Rowland LP, Shneider NA. Amyotrophic lateral sclerosis. *N Engl J Med*. 2001;344:1688–700.
3. Prell T, Lautenschläger J, Grosskreutz J. Calcium-dependent protein folding in amyotrophic lateral sclerosis. *Cell Calcium*. 2013;54:132–43.
4. Lautenschläger J, Prell T, Grosskreutz J. Endoplasmic reticulum stress and the ER mitochondrial calcium cycle in amyotrophic lateral sclerosis. *Amyotroph Lateral Scler*. 2012;13:166–77.
5. Tadic V, Prell T, Lautenschläger J, Grosskreutz J. The ER mitochondria calcium cycle and ER stress response as therapeutic targets in amyotrophic lateral sclerosis. *Front Cell Neurosci*. 2014;8:147–63.
6. Rosen DR, Siddique T, Patterson D, Figlewicz DA, Sapp P, Hentati A. Mutations in Cu/Zn superoxide dismutase gene are associated with familial amyotrophic lateral sclerosis. *Nature*. 1993;362:59–62.
7. Renton AE, Chiò A, Traynor BJ. State of play in amyotrophic lateral sclerosis genetics. *Nat Neurosci*. 2014;17:17–23.
8. Ajroud-Driss S, Siddique T. Sporadic and hereditary amyotrophic lateral sclerosis (ALS). *Biochim Biophys Acta*. 2015;1852:679–84.
9. Proctor E, Fee L, Tao Y, Redler RL, Fay J, Zhang Y, et al. Nonnative SOD1 trimer is toxic to motor neurons in a model of amyotrophic lateral sclerosis. *Proc Natl Acad Sci*. 2016;113:614–9.
10. Turner BJ, Atkin JD, Farg MA, Zang DW, Rembach A, Lopes EC, et al. Impaired extracellular secretion of mutant superoxide dismutase 1 associates with neurotoxicity in familial amyotrophic lateral sclerosis. *J Neurosci*. 2005;25:108–17.
11. Nishitoh H, Kadowaki H, Nagai A, Maruyama T, Yokota T, Fukutomi H, et al. ALS-linked mutant SOD1 induces ER stress- and ASK1-dependent motor neuron death by targeting Derlin-1. *Genes Dev*. 2008;22:1451–64.
12. Petrozziello T, Secondo A, Tedeschi V, Esposito A, Sisalli MJ, Scorziello A, et al. ApoSOD1 lacking dismutase activity neuroprotects motor neurons exposed to beta-methylamino-L-alanine through the Ca²⁺/Akt/ERK1/2 prosurvival pathway. *Cell Death Differ*. 2017;24:511–22.
13. McGuire V, Nelson LM. Epidemiology of ALS. In: Mitsumoto H, Przedborski S, Gordon PH, editors. Amyotrophic lateral sclerosis. New York: Taylor & Francis; 2006. p. 17–41.
14. Graber DJ, Harris BT. Purification and culture of spinal motor neurons from rat embryos. *Cold Spring Harb Protoc*. 2013;66:319–26.
15. Cashman N, Durham HD, Blusztajn JK, Oda K, Tabira T, Shaw IT, et al. Neuroblastoma x spinal cord (NSC) hybrid cell lines resemble developing motor neurons. *Dev Dyn*. 1992;194:209–21.

16. Secondo A, Staiano RI, Scorziello A, Sirabella R, Boscia F, Adornetto A, et al. BHK cells transfected with NCX3 are more resistant to hypoxia followed by reoxygenation than those transfected with NCX1 and NCX2: possible relationship with mitochondrial membrane potential. *Cell Calcium*. 2007;42:521–35.
17. Grynkiwicz G, Poenie M, Tsien RY. A new generation of Ca²⁺ indicators with greatly improved fluorescence properties. *J Biol Chem*. 1985;260:3440–50.
18. Urbanczyk J, Chernysh O, Condrescu M, Reeves JP. Sodium–calcium exchange does not require allosteric calcium activation at high cytosolic sodium concentrations. *J Physiol*. 2006;575:693–705.
19. Pannaccione A, Secondo A, Molinaro P, D'Avanzo C, Cantile M, Esposito A, et al. A new concept: Aβ1–42 generates a hyperfunctional proteolytic NCX3 fragment that delays caspase-12 activation and neuronal death. *J Neurosci*. 2012;32:10609–17.
20. Molinaro P, Cuomo O, Pignataro G, Boscia F, Sirabella R, Pannaccione A, et al. Targeted disruption of Na⁺/Ca²⁺ exchanger 3 (NCX3) gene leads to a worsening of ischemic brain damage. *J Neurosci*. 2008;28:1179–84.
21. Molinaro P, Viggiano D, Nisticò R, Sirabella R, Secondo A, Boscia F, et al. Na⁺–Ca²⁺ exchanger (NCX3) knock-out mice display an impairment in hippocampal long-term potentiation and spatial learning and memory. *J Neurosci*. 2011;31:7312–21.
22. Boscia F, D'Avanzo C, Pannaccione A, Secondo A, Casamassa A, Formisano L, et al. Silencing or knocking out the Na⁺/Ca²⁺ exchanger-3 (NCX3) impairs oligodendrocyte differentiation. *Cell Death Differ*. 2012;19:562–72.
23. Secondo A, Esposito A, Petrozziello T, Boscia F, Molinaro P, Tedeschi V, et al. Na⁺/Ca²⁺ exchanger 1 on nuclear envelope controls PTEN/Akt pathway via nucleoplasmic Ca²⁺ regulation during neuronal differentiation. *Cell Death Discov*. 2018;4:12–25.
24. Natale S, Anzilotti S, Petrozziello T, Ciccone R, Serani A, Calabrese L, et al. Genetic up-regulation or pharmacological activation of the Na⁺/Ca²⁺ Exchanger 1 (NCX1) enhances hippocampal-dependent contextual and spatial learning and memory. *Mol Neurobiol*. 2020;57:2358–76.
25. Bradford MM. A rapid and sensitive method for the quantitation of microgram quantities of protein utilizing the principle of protein-dye binding. *Anal Biochem*. 1976;72:248–54.
26. Adinolfi E, Callegari MG, Cirillo M, Pinton P, Giorgi C, Cavagna D, et al. Expression of the P2X7 receptor increases the Ca²⁺ content of the endoplasmic reticulum, activates NFATc1, and protects from apoptosis. *J Biol Chem*. 2009;284:10120–8.
27. Lee HC. Cyclic ADP-ribose and NAADP: fraternal twin messengers for calcium signaling. *Sci China Life Sci*. 2011;54:699–711.
28. D'Errico S, Borbone N, Catalanotti B, Secondo A, Petrozziello T, Piccialli I, et al. Synthesis and biological evaluation of a new structural simplified analogue of cADPR, a calcium-mobilizing secondary messenger firstly isolated from sea urchin eggs. *Mar Drugs*. 2018;16:89–102.
29. Sirabella R, Secondo A, Pannaccione A, Scorziello A, Valsecchi V, Adornetto A, et al. Anoxia-induced NF-κappaB-dependent upregulation of NCX1 contributes to Ca²⁺ refilling into endoplasmic reticulum in cortical neurons. *Stroke*. 2009;40:922–9.
30. Sisalli MJ, Secondo A, Esposito A, Valsecchi V, Savoia C, Di Renzo GF, et al. Endoplasmic reticulum refilling and mitochondrial calcium extrusion promoted in neurons by NCX1 and NCX3 in ischemic preconditioning are determinant for neuroprotection. *Cell Death Differ*. 2014;21:1142–9.
31. Anzilotti S, Brancaccio P, Simeone G, Valsecchi V, Vinciguerra A, Secondo A, et al. Preconditioning, induced by sub-toxic dose of the neurotoxin L-BMAA, delays ALS progression in mice and prevents Na⁺/Ca²⁺ exchanger 3 downregulation. *Cell Death Dis*. 2018;9:206–22.
32. Bartlett R, Stokes L, Sluyter R. The P2X7 receptor channel: recent developments and the use of P2X7 antagonists in models of disease. *Pharmacol Rev*. 2014;66:638–75.
33. Rakovic S, Cui Y, Iino S, Galione A, Ashamu GA, Potter BV, et al. An antagonist of cADP-ribose inhibits arrhythmogenic oscillations of intracellular Ca²⁺ in heart cells. *J Biol Chem*. 1999;274:17820–7.
34. Secondo A, Pannaccione A, Molinaro P, Ambrosino P, Lippiello P, Esposito A, et al. Molecular pharmacology of the amiloride analog 3-amino-6-chloro-5-[(4-chloro-benzyl)amino]-n-[[2,4-dimethylbenzyl]-amino] iminomethyl]-pyrazinecarboxamide (CB-DMB) as a pan inhibitor of the Na⁺–Ca²⁺ exchanger isoforms NCX1, NCX2, and NCX3 in stably transfected cells. *J Pharmacol Exp Ther*. 2009;331:212–21.
35. Diwakar L, Ravindranath V. Inhibition of cystathionine-gamma-lyase leads to loss of glutathione and aggravation of mitochondrial dysfunction mediated by excitatory amino acid in the CNS. *Neurochem Int*. 2007;50:418–26.
36. Sabri MI, Lystrup B, Roy DN, Spencer PS. Action of beta-N-oxalylamino-L-alanine on mouse brain NADH-dehydrogenase activity. *J Neurochem*. 1995;65:1842–8.
37. Valdmanis PN, Kabashi E, Dion PA, Rouleau GA. ALS predisposition modifiers: knock NOX, who's there? SOD1 mice still are. *Eur J Hum Genet*. 2008;16:140–2.
38. Apolloni S, Parisi C, Pesaresi MG, Rossi S, Carri MT, Cozzolino M, et al. The NADPH oxidase pathway is dysregulated by the P2X7 receptor in the SOD1-G93A microglia model of amyotrophic lateral sclerosis. *J Immunol*. 2013;190:5187–95.
39. Kim SU, Park YH, Min JS, Sun HN, Han YH, Hua JM, et al. Peroxiredoxin I is a ROS/p38 MAPK-dependent inducible antioxidant that regulates NF-κB-mediated iNOS induction and microglial activation. *J Neuroimmunol*. 2013;259:26–36.
40. Apolloni S, Amadio S, Parisi C, Matteucci A, Potenza RL, Armida M, et al. Spinal cord pathology is ameliorated by P2X7 antagonism in a SOD1-mutant mouse model of amyotrophic lateral sclerosis. *Dis Model Mech*. 2014;7:1101–9.
41. Ruiz-Ruiz C, Calzaferrri F, García AG. P2X7 receptor antagonism as a potential therapy in amyotrophic lateral sclerosis. *Front Mol Neurosci*. 2020;13:93–105.
42. Mühling T, Duda J, Weishaupt JH, Ludolph AC, Liss B. Elevated mRNA-levels of distinct mitochondrial and plasma membrane Ca(2+) transporters in individual hypoglossal motor neurons of endstage SOD1 transgenic mice. *Front Cell Neurosci*. 2014;8:353–66.
43. Clapper DL, Walseth TF, Dargie PJ, Lee HC. Pyridine nucleotide metabolites stimulate calcium release from sea urchin egg microsomes desensitized to inositol trisphosphate. *J Biol Chem*. 1987;262:9561–8.
44. Thai TL, Arendshorst WJ. Mice lacking the ADP ribosyl cyclase CD38 exhibit attenuated renal vasoconstriction to angiotensin II, endothelin-1, and norepinephrine. *Am J Physiol Renal Physiol*. 2009;297:F169–76.
45. Formisano L, Saggese M, Secondo A, Sirabella R, Vito P, Valsecchi V, et al. The two isoforms of the Na⁺/Ca²⁺ exchanger, NCX1 and NCX3, constitute novel additional targets for the prosurvival action of Akt/protein kinase B pathway. *Mol Pharmacol*. 2008;73:727–37.
46. Sirabella R, Secondo A, Pannaccione A, Molinaro P, Formisano L, Guida N, et al. ERK1/2, p38, and JNK regulate the expression and the activity of the three isoforms of the Na⁺/Ca²⁺ exchanger, NCX1, NCX2, and NCX3, in neuronal PC12 cells. *J Neurochem*. 2012;122:911–22.
47. Molinaro P, Pannaccione A, Sisalli MJ, Secondo A, Cuomo O, Sirabella R, et al. A new cell-penetrating peptide that blocks the autoinhibitory XIIP domain of NCX1 and enhances antiporter activity. *Mol Ther*. 2015;23:465–76.
48. Martelli AM, Tabellini G, Bressanin D, Ognibene A, Goto K, Cocco L, et al. The emerging multiple roles of nuclear Akt. *Biochim Biophys Acta*. 2012;1823:2168–78.
49. Ruegsegger C, Maharjan N, Goswami A, Filézac de L'Etang A, Weis J, et al. Aberrant association of misfolded SOD1 with Na(+)/K(+)ATPase-α3 impairs its activity and contributes to motor neuron vulnerability in ALS. *Acta Neuropathol*. 2016; 131:427–51.
50. Saxena S, Roselli F, Singh K, Leptien K, Julien JP, Gros-Louis F, et al. Neuroprotection through excitability and mTOR required in ALS motoneurons to delay disease and extend survival. *Neuron*. 2013;80:80–96.

Publisher's Note

Springer Nature remains neutral with regard to jurisdictional claims in published maps and institutional affiliations.